Temperature-dependent critical currents in superconducting $YBa_2Cu_3O_{7-\delta}$ and ferromagnetic $La_{2/3}Ca_{1/3}MnO_3$ hybrid structures

M. Djupmyr,[1] S. Soltan,[2] H.-U. Habermeier,[2] and J. Albrecht[1,3]
[1]*Max-Planck-Institut für Metallforschung, Heisenbergstr. 3, D-70569 Stuttgart, Germany*
[2]*Max-Planck-Institut für Festkörperforschung, Heisenbergstr. 1, D-70569 Stuttgart, Germany*
[3]*Hochschule Aalen, Beethovenstr. 1, D-73430 Aalen, Germany*
(Received 2 July 2009; revised manuscript received 16 October 2009; published 17 November 2009)

The local critical current density in thin-film hybrid structures of high-temperature superconducting $YBa_2Cu_3O_{7-\delta}$ and ferromagnetic $La_{2/3}Ca_{1/3}MnO_3$ (LCMO) is measured with high accuracy using a quantitative magneto-optical method. The superconducting films are grown onto vicinal cut substrates where step-flow growth creates a highly ordered microstructure including an array of parallel oriented planar defects. This generates an anisotropy of the critical current in the superconductor, arising from the different values of the current density depending on whether it has to flow across the defects or not. The addition of an LCMO layer leads to an increase of the current anisotropy meaning that the two nonequivalent current directions are affected by the stray field of the adjacent ferromagnet in different ways. The magnetization of the ferromagnetic LCMO is mainly in-plane oriented but exhibits finite out-of-plane components originated from a high density of Néel-type domain walls. Performing temperature-dependent measurements of the critical current density from $T=7$ K to $T=90$ K and comparing with results from YBCO single layers, the influence of the ferromagnet on the critical current density is studied in detail. It is found that depending on the defect structure of the current path the critical currents are affected in different ways by the ferromagnet. The comparison of single layer superconducting films and heterostructures in conjunction with the realized different microstructure along the current path inside one individual sample, allows the identification of the current transport mechanisms in YBCO thin films and how they are influenced by the magnetic stray fields from the added LCMO layer.

DOI: 10.1103/PhysRevB.80.184507 PACS number(s): 74.25.Fy, 74.72.Bk, 74.78.Bz, 74.78.Fk

I. INTRODUCTION

The large anisotropy in high-temperature superconductors combined with the unconventional symmetry of the order parameter lead to a strong influence of the microstructure on the electrical transport properties.[1–3] The highest critical current densities are found in epitaxially grown thin films.[4] These films can combine a high degree of crystallographic order with an appropriate defect structure for effective flux-line pinning. The origin of flux-line pinning is a spatial variation of the flux-line energy inside the superconductor. This leads to preferred positions of the flux lines where the motion is hindered even under acting Lorentz forces created by transport currents. The decisive properties for vortex pinning are the total-energy gain which is mainly governed by the condensation energy of the superconducting (SC) state and the shape of the pinning potential since its gradient defines the pinning force. To maximize a possible energy gain, a highly ordered microstructure is required, which explains the need of an epitaxial film. To realize high pinning forces the available pinning energy has to exhibit large changes on short length scales. Since for high-temperature superconductors, the London penetration depth λ is much larger than the coherence length ξ, the dominant contributions to the pinning force density usually arise from vortex core pinning of flux lines. To generate effective pinning centers, normal conducting defects need to have a size comparable to the order of ξ, which for $YBa_2Cu_3O_{7-\delta}$ is about 2 nm at low temperatures. Such effective pinning sites can be screw dislocations,[5] step dislocations,[6] or oxygen vacancies.[7]

Temperature-dependent measurements of the critical current allow identification of the pinning mechanisms important for current transport in thin films with different microstructure.[8–10] Especially, the local critical current density in $YBa_2Cu_3O_{7-\delta}$ (YBCO) thin films can be described using power-law functions of the reduced temperature $t=1-T/T_c$. While in general a linear current-temperature relation is observed at temperatures above $T=40$ K, the power-law exponent at lower temperatures is strongly dependent on the microstructure of the superconducting film.[11] YBCO films with nearly defect-free current paths, can be described by a current-temperature relation of $j \propto (1-T/T_c)^{3/2}$ in the significant temperature regime $15<T<40$ K.[12] This exponent $s=3/2$ is found theoretically, when considering strong individual flux-line pinning at the length scale of the coherence length ξ.[11–13] However, the microstructure of thin films of high-temperature superconductors is strongly dependent on the substrate used and for most substrates there is an island growth occurring. This results in films with growth islands the size of several 100 nm and a high density of low-angle grain boundaries acting as inhomogeneities along the current path. Such YBCO thin films have been thoroughly investigated and the temperature dependence of the critical current show an exponent s that is significantly larger than the theoretical value of 3/2.[11] Films with very few microstructural inhomogeneities can be prepared by changing the growth mode. This can be done by using a vicinal cut substrate, which is a substrate with a regular step and terrace surface structure. Here a step-flow growth of YBCO will take place which results in a very smooth film nearly without grain

boundaries along the steps.[14] Further vicinal films benefit from having different microstructure along and across the steps of the substrate leading to different current properties that can be measured at the same time using magneto-optics.

The electrical transport in such highly ordered YBCO films with an additional interface to a ferromagnet will be the main topic of this paper. The addition of a ferromagnetic layer on top of the superconductor is expected to give a possibility to explore contributions of magnetic pinning but also to enable new insights into the current limiting mechanisms of the superconductor. To enable the study of such a complex bilayer, it is important to use a well defined system including microstructure. Therefore a YBCO film exhibiting a large mean-free path in the direction of the current flow is combined with a ferromagnetic layer of $La_{2/3}Ca_{1/3}MnO_3$ (LCMO) to form a ferromagnet-superconductor hybrid structure. The ferromagnetic layer is expected to strongly influence the properties of the superconducting YBCO thin film,[15–17] for example, leading to reduced critical temperature T_c. The purpose of this work is therefore, to explore the consequences of an adjacent ferromagnetic layer for the critical current in a YBCO thin film with well defined defect structure.

II. HYBRID STRUCTURES

To investigate to what extent the mutual interaction between both materials leads to a change in the electrical transport properties of the superconductor, a detailed study of the temperature dependence of the critical current in a superconductor/ferromagnet bilayer will be presented and a comparison made to the properties of single layer YBCO thin films with identical microstructure. First, we realize a nearly homogeneous current path, by growing a film onto a vicinal cut substrate, characterized by a regular step and terrace surface structure. Due to this special structure a step-flow growth of the YBCO is occurring, producing a very homogeneous film without growth islands along the steps. Between the steps a stacking mismatch of the YBCO lattice results in nearly parallel antiphase boundaries. These are elongated along the steps and parallel to the c-axes and thus act as effective pinning centers. This particular microstructure generates a strongly anisotropic critical current j_c, reaching much higher values for the longitudinal current path flowing along the steps than the transversal that has to pass across the antiphase boundaries. Second, a highly regular, electronically as well as magnetically, interface to a ferromagnet is required. We use LCMO since it has similar crystal structure and lattice parameters as YBCO, enabling epitaxial growth with atomically flat interfaces.[18] High-quality interfaces are important for the study of coupling effects between ferromagnet and superconductor, to allow the diffusion of Cooper pairs and spin-polarized quasiparticles across the interface.[19] Due to the growth under tensile strain the preferred magnetization direction of the LCMO layer is in the plane of the film.[20–22] Nevertheless, components of out-of-plane magnetization has been observed with local scanning hall probe microscopy (SHPM) measurements of YBCO films of comparable thickness grown on top of LCMO.[23] These originate from Néel-type walls that are formed between magnetic domains or possibly local out-of-plane domains. Further a magnetic anisotropy has been observed in ultra thin LCMO films grown on vicinal substrates.[24]

The films studied were grown epitaxially onto vicinal cut $SrTiO_3$ substrates with a nominal vicinal angle $\theta=10°$, using pulsed laser deposition. The YBCO is optimally doped, 150 nm thick and a bilayer is formed by adding 50 nm LCMO on top of it. The lateral size of the films is 5×5 mm^2.

III. TEMPERATURE-DEPENDENT MEASUREMENTS

Since the critical current is anisotropic in these films, it is necessary to use an experimental method that is able to access local data for different current directions. This is accomplished by applying the magneto-optical Faraday effect, producing images of the magnetic-flux density distribution in the film. From these images the critical current-density distribution j_c can be calculated using an inversion of the Biot-Savart law in two dimensions, being a good approximation for thin films. In this process an iteration method developed by Laviano *et al.*[25] is applied to omit errors caused by in-plane magnetic fields. As a result gray scale images of j_c can be obtained with a spatial resolution of better than 5 μm.[26]

In our experiments the magnetic-flux distribution of the remanent state was measured as a function of temperature. In detail this means the films were cooled down to $T=7$ K. Next an external field of $\mu_0 H=250$ mT was applied for several seconds to assure full vortex penetration. Removing the field finally puts the film into the remanent state. Relaxation processes of the flux lines are kept small by waiting several minutes[27] before taking the first image and using a constant delay time of 10 s before each of the following images. In this way the images are really showing the pinned magnetic-flux distribution. Images were taken at increasing temperatures from 7 K up to above $T_c=81$ K for the bilayer and $T_c=91$ K for the YBCO thin film.

Four images of critical current-density distributions are presented in Fig. 1, where (a) and (c) are showing the YBCO thin film and (b) and (d) the bilayer at $T=20$ K and $T=50$ K, respectively. The gray scale refers to current densities of 0 (black) up to 3×10^{11} A/m^2 (white). The current in square shaped high quality thin films is flowing in rectangular loops parallel to the film edges,[28] forming four domains of currents with constant magnitude and direction. This allows the analysis of currents along and perpendicular to the steps in the same measurement.

IV. ANISOTROPY

Films grown on vicinal cut substrates exhibit an anisotropic critical current density with two of the domains having significantly higher currents. The strong current anisotropy can be clearly seen in the images. The longitudinal (L) critical current $j_{c,L}$ flowing along the steps seen as bright areas is much higher than the transversal (T) $j_{c,T}$ that has to flow across the steps seen as dark gray areas and indicated by arrows in Fig. 1(a). Both films are grown on the same type of vicinal substrates, the only difference is the added ferromag-

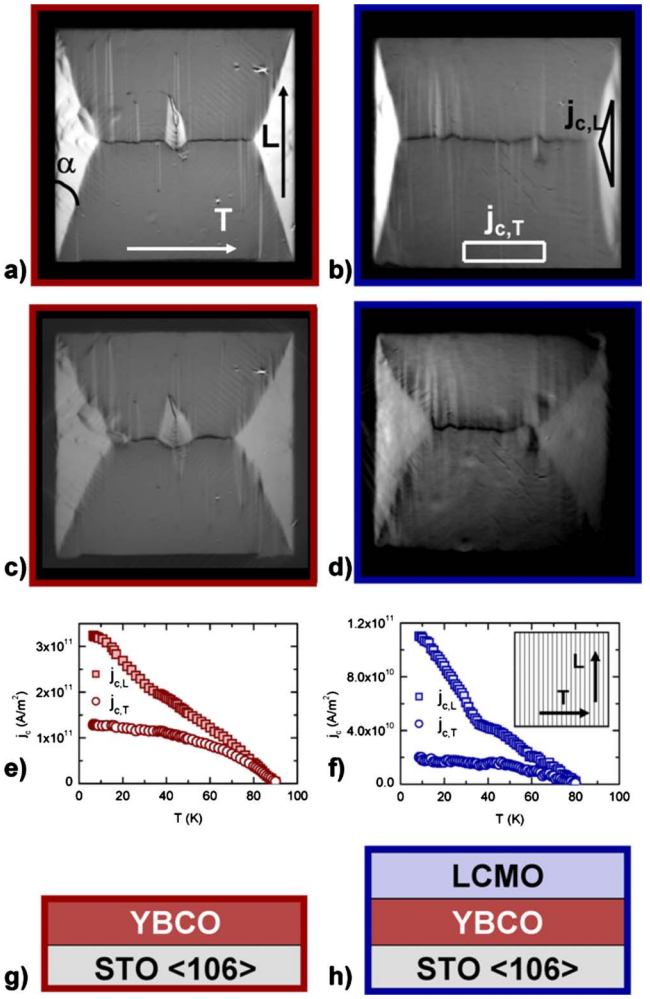

FIG. 1. (Color online) Critical current-density distribution at $T=20$ K in (a) a YBCO thin film and b) a bilayer of YBCO and LCMO, and at $T=50$ K (c) and (d), respectively. Both films are grown onto vicinal cut STO substrates. The bilayer shows a larger anisotropy. (e) and (f) show the temperature dependences of the critical currents $j_{c,L}$ and $j_{c,T}$ for each film. (g) show the structure of the YBCO film and (h) the structure of the bilayer.

netic layer on top of the superconductor for the bilayer and therefore no difference in microstructure of the superconducting layer in the two films is expected. Sketches of the structure of the YBCO thin film is shown Fig. 1(g) and the bilayer in Fig. 1(h). Nevertheless, a comparison reveals, apart from reduced currents, also a significantly enhanced anisotropy in the bilayer [Fig. 1(b)]. Using the angle α [see Fig. 1(a)] between areas with different current direction the anisotropy can be calculated as $A_\alpha = 1/\tan\alpha$,[26] where $A_\alpha = 2.4$ for the YBCO thin film and $A_\alpha = 4.2$ for the bilayer at $T=20$ K. This means that the addition of the ferromagnetic layer almost doubles the anisotropy at this temperature and that currents in different directions must be affected in different ways by the ferromagnet. The anisotropy can also be determined from local values of the critical current, calculated independently for each current direction.[26] This is done by averaging over areas with side lengths of several 100 μm indicated in Fig. 1(b). The areas were chosen around the $B=0$ line[29] as to take care of any field dependence of the

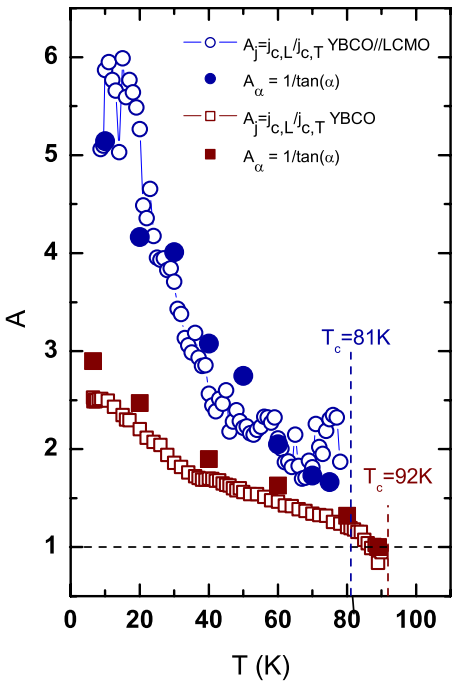

FIG. 2. (Color online) Temperature dependence of the anisotropy $j_{c,L}/j_{c,T}$ in the YBCO thin film (□) and in the bilayer (○). The filled symbols are calculated from the angle between areas with different current direction.

critical current that might occur due to flux-line flux-line interactions. These carefully obtained values for the critical current were obtained for each temperature and are plotted in Figs. 1(e) and 1(f) for the YBCO film and the bilayer, respectively. In both plots squares show the temperature dependence of the longitudinal critical current flowing along the steps and circles that of the transversal current flowing across the steps of the substrate, see the sketch of the substrate in the inset of Fig. 1(f). A very different temperature dependence of the two current directions is found in both films and is origin of the current anisotropy. But there is also a big difference in the behavior between the single layer and the bilayer.

The current anisotropy can thus also be calculated from the values of $j_{c,L}$ and $j_{c,T}$ and is defined as $A_j = j_{c,L}/j_{c,T}$. Figure 2 shows the anisotropy vs temperature for the YBCO single layer(squares) and for the bilayer(circles). The open and filled symbols refer to results obtained from the geometric and the current ratio analysis, respectively. Note that both methods lead to corresponding results, which gives evidence that quantitative magneto-optical imaging can be applied to ferromagnet-superconductor hybrids.[30] The data of Fig. 2 show that the anisotropy of the bilayer is strongly enhanced, especially at low temperatures, where it is about twice that of the YBCO single layer and this although the superconducting layers have the same microstructure. This suggests that the critical current is affected by the ferromagnet in a different way along different directions. In other words, the critical current in YBCO/LCMO bilayers is much more sensitive to the microstructure along the current path than is the individual YBCO film. Figure 2 shows further that different temperature dependences are found for the anisotropy in the two

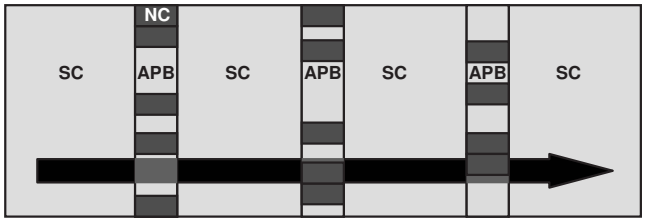

FIG. 3. The transversal current is flowing across the antiphase boundaries. Thereby it has to cross regions with reduced superconductivity (APB) separating highly SC islands. The APBs consists of SC and nonsuperconducting (NC) regions.

films. In the bilayer it decreases more steeply especially for temperatures up to $T \approx 40$ K. Also notably is that in the bilayer, a substantial anisotropy is still found for temperatures close to T_c.

V. TEMPERATURE-DEPENDENT CRITICAL CURRENTS

Understanding this behavior requires an understanding of $j_c(T)$ along the two different current directions, $j_{c,T}(T)$ and $j_{c,L}(T)$. The limiting factors of these currents are completely different because of different microstructures along the current paths.[9,31] For the T direction the current has to pass through an array of antiphase boundaries that is arising from the substrate steps, while the L direction exhibits a highly transparent, nearly grain-boundary-free current path. Therefore the two current directions have to be treated separately when looking at the mechanisms of the critical currents.

For the L direction $j_{c,L}$ can be described by a power law,

$$j_c(T) = j_c(0)\left(1 - \frac{T}{T_c}\right)^s. \tag{1}$$

The exponent s changes at $T \approx 40$ K and we can distinguish between two temperature regimes with different pinning mechanisms. At temperatures above 40 K thermally activated depinning of flux lines is limiting the current and an exponent of $s=1$ is found. At temperatures below 40 K the exponent $s=1.5$ proves effective and strong vortex core pinning enabling the observed high currents.[11]

The current direction perpendicular to the substrate steps, $j_{c,T}$, can be treated like a current which flows along an array of superconducting islands with excellent transport properties which are separated by regions of high disorder, high scattering rates and poor transport properties. A simple model describing this scenario is depicted in Fig. 3. Here the superconducting islands indicated SC are separated by the weakly superconducting regions of size ξ created by the antiphase boundaries (APBs). Already in 1987 Deutscher and Müller[32,33] suggested that such narrow planar defects can be treated as Josephson junctions with depressed order parameter Δ. The Josephson coupling current is described by the model of Ambegaokar and Baratoff. But since it is originally describing a BCS superconductor it needs to be adjusted before it can be applied to the present HTSC system. Therefore a modified Ambegaokar-Baratoff function will be proposed which takes the depression of the order parameter into account. This leads to the following temperature dependence of the critical current density:

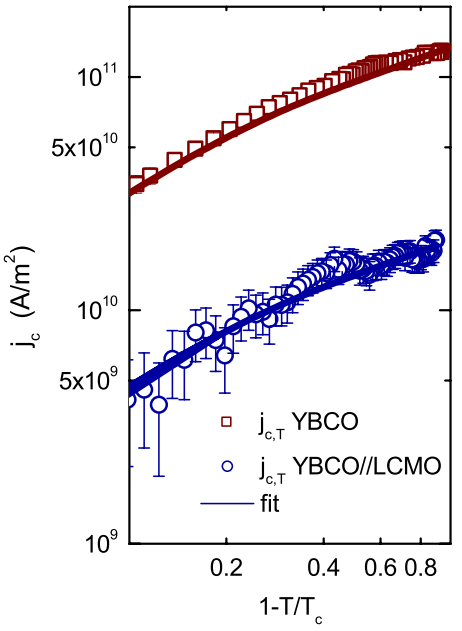

FIG. 4. (Color online) Temperature dependence of the transversal critical currents $j_{c,T}$ in the YBCO thin film (□) and the bilayer (○). The solid lines represent fits to the model of Ambegaokar and Baratoff.

$$j(T) = j(0)\sqrt{1 - \frac{T}{T_c}}\tanh\left(\frac{A\sqrt{1 - \frac{T}{T_c}}}{\frac{T}{T_c}}\right). \tag{2}$$

In this equation the depression of the order parameter is included in $j(0)$ and A that will be used as fitting parameters when employing the equation to describe measured data.

For oxide superconductor/ferromagnet hybrids, it is known that there is generally a suppression of critical currents and transition temperatures originating in coupling effects of the counteractive ordering phenomena.[15,17] The interactions take place in several ways, through oxygen diffusion,[34] charge transfer,[35] redistribution of orbital occupancy,[36] spin diffusion,[17,37] and dipolar coupling via stray fields. Since the first three effects are limited to a thin layer at the interfaces they will not substantially influence the properties of a thicker film of several 100 μm. This is different for the two last effects[38] where the coupling of magnetic stray fields of the vortex systems and domain pattern in the constituents can lead to a substantial magnetic-flux-line pinning.[23,39]

VI. RESULTS

The temperature dependence of the critical currents will now be presented for each current direction separately, starting with $j_{c,T}$. The data are plotted in a double-logarithmic scale in Fig. 4, squares denote the values for the YBCO thin film and circles the bilayer. The errors are estimated not to be

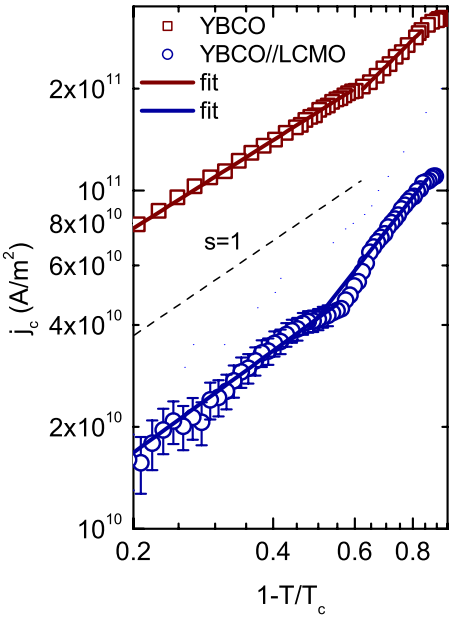

FIG. 5. (Color online) Temperature dependence of the longitudinal critical current densities $j_{c,L}$ in YBCO (□) and the bilayer (○). The lines represent fits to the power law $j_c(T)=j_c(0)(1-T/T_c)^s$.

larger than 3×10^9 A/m^2 and are included in the figure, though for the YBCO thin film they are smaller than the used symbols. The solid lines are fits to Eq. (2). We find a strong suppression of the critical current in the bilayer by a factor of about 7. The importance of Fig. 4 is twofold. First, the temperature dependence does not change due to the general suppression of j_c. Second, all data can be fitted to the modified Ambegaokar-Baratoff function which although a simple model give a surprisingly accurate description.

This is different for the longitudinal current component $j_{c,L}$ that is depicted in Fig. 5. Again, squares denote the YBCO thin film and circles the bilayer. The experimental data can now be fitted to Eq. (1) using $j_c(0)$ and s as free parameters. For temperatures above $T=40$ K up to T_c both curves show an exponent close to $s=1$ and no change in the temperature dependence can be seen due to the ferromagnetic layer. At $T\approx40$ K the temperature-dependence changes for both samples and in case of the vicinal YBCO thin film we find an exponent $s=1.4\pm0.1$. A larger exponent s, meaning a stronger decay of the currents with temperature, is found in case of the bilayer. In addition to that, the current suppression by a factor of 3–4 is much weaker than for the transversal current $j_{c,T}$. This directly gives rise to the different anisotropy values that are found, presented in Fig. 2.

To more clearly envision the behavior at temperatures below $T=40$ K, the currents are plotted with higher magnification and normalized to their values at $T=13$ K in Fig. 6. A temperature of $T=13$ K is chosen because at lower temperatures quantum creep of flux lines lead to a deviation from the power law.[12] The critical current of the bilayer, denoted by circles, is decreasing more steeply with temperature than for the YBCO single layer, denoted by squares. An exponent $s=1.8\pm0.1$ is found for the bilayer, substantially larger than $s=1.4\pm0.1$ found for the YBCO thin film.

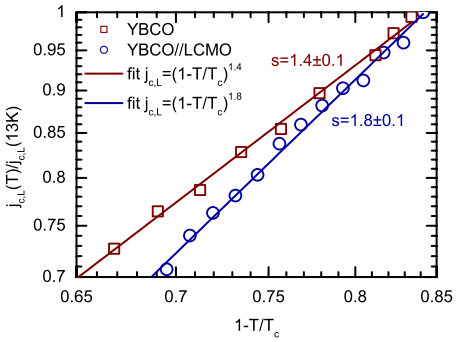

FIG. 6. (Color online) Temperature dependence of the longitudinal critical currents $j_{c,L}$ normalized to the values at $T=13$ K in YBCO (□) and the bilayer (○) The lines are fits to $(1-T/T_c)^s$ with $s=1.4$ and $s=1.8$, respectively.

VII. DISCUSSION

After showing the experimental results, we will now discuss the role of the ferromagnetic layer on the current transport mechanisms in the superconductor. For $j_{c,T}$ a temperature dependence was found for both films which could be described by the modified Ambegaokar and Baratoff function, Eq. (2). Assuming Josephson coupling across the APBs, a modulation of the critical current by magnetic field is also to be expected. For a single Josephson junction the magnetic field dependence of the tunneling current is given by the second Josephson equation,

$$j_{c,T}(B) = j_{c,T}(0)\cdot\left|\frac{\sin\left(\frac{\pi\Phi}{\Phi_0}\right)}{\frac{\pi\Phi}{\Phi_0}}\right|, \tag{3}$$

with $\Phi=2\lambda_L lB$ and l the size of the contact perpendicular to the magnetic field.

Already a small magnetic field, as the stray fields from the ferromagnet, will suppress the critical current substantially. The structure of a APB though is not expected to be as simple as one single planar defect. Instead it is expected that each APB contain numerous defects of size ξ and smaller. If the defects are large enough with respect to ξ they can locally cause disruptions in the current flow. It is therefore more correct to think of the APB as built up of superconducting and nonsuperconducting regions as depicted in Fig. 3. Bernstein *et al.*[40] suggested that planar defects split up in structures that locally behave like Josephson weak links or superconducting-quantum-interference-device (SQUID)-like structures. Since along the whole length of the APB there are all kind of defect structures expected, it is difficult to make an exact description. Nevertheless the above discussion can explain the simultaneously observed tunneling characteristic and high critical currents found in the presented measurements.

Now the $j_{c,L}$ will be discussed. It can be described as a pinning dominated current that in case of the YBCO single layer, for $T<40$ K, can be described by[13]

$$j_c(T) = \frac{c}{\phi_0} f_{pin}^{max} = \frac{9}{32}\sqrt{\frac{2}{3}}\frac{c}{\phi_0}\frac{\epsilon_0}{\xi} \propto \left(1 - \frac{T}{T_c}\right)^{3/2}. \quad (4)$$

The exponent $s=3/2$ can only bee found for a grain-boundary-free current, as along the steps in vicinal films, while additional inhomogeneities are known to increase the exponents.[11]

Analyzing the temperature-dependent currents along the L-direction in the bilayer, we again find a power-law description of the data and surprisingly, an exponent $s=1.8$ for $T<40$ K, which is significantly larger than $s=3/2$. This is remarkable because the microstructure of the YBCO constituent of the bilayer should be the same as for the compared individual layer since the ferromagnet has been grown on top.

If an increase of the exponent s refers to an increased inhomogeneity of the current path, we could interpret our results in terms of a magnetically induced inhomogeneity. To follow this idea we have to refer to superconducting systems with granular character where a shift of the magnetization maximum to finite fields is found when measuring the field dependent magnetization.[41] The same effect has been found in LCMO/YBCO hybrid structures where the layers have been electronically decoupled by thin insulating barriers.[39] Owing to the high critical currents in the latter case the presence of weak links can be denied, which also holds for the samples considered in this work. SHPM measurements of YBCO films of comparable thickness grown on top of LCMO show that an inhomogeneous magnetic stray field with varying in-plane and out-of-plane components penetrates the superconductor over its whole thickness of 100 nm or above.[23] These experimental facts, namely the shift of the magnetization maximum toward finite fields, the inhomogeneous magnetic field pattern in a YBCO film on top of an LCMO film and finally the increase of the power-law exponent s measured in this work allow only one conclusion. The transport of supercurrents in all-oxide superconductor-ferromagnet hybrids has to be described as inhomogeneous transport, where the local magnetic field penetrating into the superconducting film creates magnetic obstacles for the current flow. This scenario allows the indirect realization of magnetically controlled flux-line pinning in high-temperature superconductors, this through changes in magnetization of the manganite which can be accessed via external magnetic fields.

VIII. CONCLUSIONS

In summary, we have investigated critical current densities in epitaxial hybrids of superconducting YBCO and ferromagnetic LCMO. Using quantitative magnetooptics in conjunction with films on vicinal cut substrates allowed the independent analysis of currents flowing along current paths with different microstructures. Comparing the results with currents flowing in YBCO single layers we have found that the influence of the adjacent ferromagnetic layer on the critical currents strongly depend on the microstructure. In case of currents across planar defects such as antiphase boundaries we observe a tunnelinglike behavior which is very sensitive to the presence of magnetic stray fields. This influence is noticed to be temperature independent. The combined findings of high critical currents and tunneling character can be modeled by introducing structures locally behaving like Josephson weak links. Along the highly homogeneous current path, realized along the surface steps of the substrate, there is a completely different temperature dependence. Here, it is discovered that the adjacent ferromagnet is causing a stronger decrease of the critical current with temperature, compared to YBCO single layers with identical microstructure. This current transport can be described as inhomogeneous where one reason for the inhomogeneity is the stray field distribution of the ferromagnet penetrating the superconductor.

ACKNOWLEDGMENTS

The authors are grateful to Georg Cristiani for producing the excellent samples. Further we would like to thank Sebastian Treiber for helpful discussion and comments.

[1] D. Dimos, P. Chaudhari, J. Mannhart, and F. K. LeGoues, Phys. Rev. Lett. **61**, 219 (1988).
[2] C. Gerber, D. Anselmetti, J. G. Bednorz, J. Mannhart, and D. G. Schlom, Nature (London) **350**, 279 (1991).
[3] D. J. Van Harlingen, Rev. Mod. Phys. **67**, 515 (1995).
[4] B. Dam *et al.*, Nature (London) **399**, 439 (1999).
[5] J. Mannhart, D. Anselmetti, J. Bednorz, A. Cantana, C. Gerber, K. Müller, and D. Schlom, Z. Phys. B **86**, 177 (1992).
[6] A. Gurevich and L. D. Cooley, Phys. Rev. B **50**, 13563 (1994).
[7] H. Theuss and H. Kronmüller, Physica C **177**, 253 (1991).
[8] H. Yan, M. M. Abdelhadi, J. A. Jung, B. A. Willemsen, and K. E. Kihlstrom, Phys. Rev. B **72**, 064522 (2005).
[9] C. Jooss, R. Warthmann, H. Kronmüller, T. Haage, H.-U. Habermeier, and J. Zegenhagen, Phys. Rev. Lett. **82**, 632 (1999).
[10] J. Gutiérrez *et al.*, Nature Mater. **6**, 367 (2007).
[11] J. Albrecht, M. Djupmyr, and S. Brück, J. Phys.: Condens. Matter **19**, 216211 (2007).
[12] M. Djupmyr, G. Cristiani, H.-U. Habermeier, and J. Albrecht, Phys. Rev. B **72**, 220507(R) (2005).
[13] V. Pan, Y. Cherpak, V. Komashko, S. Pozigun, C. Tretiatchenko, A. Semenov, E. Pashitskii, and A. Pan, Phys. Rev. B **73**, 054508 (2006).
[14] J. Brötz, H. Fuess, T. Haage, and J. Zegenhagen, Phys. Rev. B **57**, 3679 (1998).
[15] Z. Sefrioui, D. Arias, V. Peña, J. E. Villegas, M. Varela, P. Prieto, C. León, J. L. Martinez, and J. Santamaria, Phys. Rev. B **67**, 214511 (2003).
[16] P. Przyslupski, I. Komissarov, W. Paszkowicz, P. Dluzewski, R. Minikayev, and M. Sawicki, Phys. Rev. B **69**, 134428 (2004).
[17] S. Soltan, J. Albrecht, and H.-U. Habermeier, Phys. Rev. B **70**,

144517 (2004).
[18] H.-U. Habermeier, G. Cristiani, R. Kremer, O. Lebedev, and G. V. Tendeloo, Physica C **364-365**, 298 (2001).
[19] F. S. Bergeret, A. F. Volkov, and K. B. Efetov, Rev. Mod. Phys. **77**, 1321 (2005).
[20] C. Kwon *et al.*, J. Magn. Magn. Mater. **172**, 229 (1997).
[21] A. M. Haghiri-Gosnet, J. Wolfman, B. Mercey, C. Simon, P. Lecoeur, M. Korzenski, M. Hervieu, R. Desfeux, and G. Baldinozzi, J. Appl. Phys. **88**, 4257 (2000).
[22] Q. Lu, C.-C. Chen, and A. de Lozanne, Science **276**, 2006 (1997).
[23] J. Albrecht, M. Djupmyr, S. Soltan, H.-U. Habermeier, M. Connolly, and S. Bending, New J. Phys. **9**, 379 (2007).
[24] Z.-H. Wang, G. Cristiani, and H.-U. Habermeier, Appl. Phys. Lett. **82**, 3731 (2003).
[25] F. Laviano, D. Botta, A. Chiodoni, R. Gerbaldo, G. Ghigo, L. Gozzelino, S. Zannella, and E. Mezzetti, Supercond. Sci. Technol. **16**, 71 (2003).
[26] C. Jooss, J. Albrecht, H. Kuhn, S. Leonhardt, and H. Kronmüller, Rep. Prog. Phys. **65**, 651 (2002).
[27] R. Warthmann, J. Albrecht, H. Kronmüller, and C. Jooss, Phys. Rev. B **62**, 15226 (2000).
[28] T. Schuster, M. V. Indenbom, M. R. Koblischka, H. Kuhn, and H. Kronmüller, Phys. Rev. B **49**, 3443 (1994).
[29] T. Schuster, M. Koblischka, H. Kuhn, B. Ludescher, M. Leghissa, M. Lippert, and H. Kronmüller, Physica C **196**, 373 (1992).
[30] J. Albrecht, S. Soltan, and H.-U. Habermeier, Europhys. Lett. **63**, 881 (2003).
[31] T. Haage, J. Zegenhagen, J. Q. Li, H.-U. Habermeier, M. Cardona, C. Jooss, R. Warthmann, A. Forkl, and H. Kronmüller, Phys. Rev. B **56**, 8404 (1997).
[32] G. Deutscher and K. A. Müller, Phys. Rev. Lett. **59**, 1745 (1987).
[33] G. Deutscher, IBM J. Res. Dev. **33**, 293 (1989).
[34] R. A. Chakalov, G. Passerieux, I. P. Jones, P. Mikheenko, J. Ireland, R. I. Chakalova, M. S. Colclough, and C. M. Muirhead, J. Appl. Phys. **98**, 123908 (2005).
[35] M. Varela, A. R. Lupini, S. J. Pennycook, Z. Sefrioui, and J. SantamariaSolid-State Electron. **47**, 2245 (2003).
[36] J. Chakhalian *et al.*, Nat. Phys. **2**, 244 (2006).
[37] H.-U. Habermeier, S. Soltan, and J. Albrecht, Physica C **460-462**, 32 (2007).
[38] S. Soltan, J. Albrecht, and H.-U. Habermeier, Mater. Sci. Eng., B **144**, 15 (2007).
[39] J. Albrecht, S. Soltan, and H.-U. Habermeier, Phys. Rev. B **72**, 092502 (2005).
[40] P. Bernstein, Y. Bougherira, J. Hamet, Y. Thimont, and L. Me'chin, Phys. Rev. B **78**, 054517 (2008).
[41] D. V. Shantsev, M. R. Koblischka, Y. M. Galperin, T. H. Johansen, L. Půst, and M. Jirsa, Phys. Rev. Lett. **82**, 2947 (1999).